2-14-2004

Post-Acquisition Small-Animal Respiratory Gated Imaging Using Micro Cone-Beam CT

Jicun Hu
Marquette University

Steven Thomas Haworth
Medical College of Wisconsin

Robert C. Molthen
Marquette University, robert.molthen@marquette.edu

Christopher A. Dawson
Medical College of Wisconsin

Published version. Published as part of the proceedings of the conference, *SPIE 5369: Medical Imaging 2004: Physiology, Function, and Structure from Medical Images*, 2004: 350-360. DOI.

Post Acquisition Small Animal Respiratory Gated Imaging Using micro Cone-Beam CT

Jicun Hu[a], Steve T. Haworth[b], Robert C. Molthen[a,b,c], and Christopher A. Dawson[a,b,c]

[a]Department of Biomedical Engineering, Marquette University, Milwaukee, WI 53203
[b]Department of Physiology, Medical College of Wisconsin, Milwaukee, WI, 53226
[c]Zablocki VA Medical Center, Milwaukee, WI, 53295

ABSTRACT

On many occasions, it is desirable to image lungs *in vivo* to perform a pulmonary physiology study. Since the lungs are moving, gating with respect to the ventilatory phase has to be performed in order to minimize motion artifacts. Gating can be done in real time, similar to cardiac imaging in clinical applications, however, there are technical problems that have lead us to investigate different approaches. The problems include breath-to-breath inconsistencies in tidal volume, which makes the precise detection of ventilatory phase difficult, and the relatively high ventilation rates seen in small animals (rats and mice have ventilation rates in the range of a hundred cycles per minute), which challenges the capture rate of many imaging systems (this is particularly true of our system which utilizes cone-beam geometry and a 2 dimensional detector). Instead of pre-capture ventilation gating we implemented a method of post-acquisition gating. We acquire a sequence of projections images at 30 frames per second for each of 360 viewing angles. During each capture sequence the rat undergoes multiple ventilation cycles. Using the sequence of projection images, an automated region of interest algorithm, based on integrated grayscale intensity, tracts the ventilatory phase of the lungs. In the processing of an image sequence, multiple projection images are identified at a particular phase and averaged to improve the signal-to-ratio. The resulting averaged projection images are input to a Feldkamp cone-beam algorithm reconstruction algorithm in order to obtain isotropic image volumes. Minimal motion artifact data sets improve qualitative and quantitative analysis techniques useful in physiologic studies of pulmonary structure and function.

Keywords: X-ray, micro-CT, respiratory gating, cone-beam, small animal imaging

1. INTRODUCTION

Small animal imaging has been an active research field recently since small animal models, such as rats or mice, can be used to study the mechanisms of different important diseases in human[1]. To obtain high sensitivity and resolution in small animal imaging, dedicated micro imaging systems have to be developed. Currently, these imaging systems include micro-MR[2], micro SPECT[3,4], micro PET[5], and micro CT[6-9], each having their own advantages and disadvantages. In order to combine the strength of different modalities, hybrid imaging systems have been developed[10,11]. Micro cone beam CT, as a powerful and relatively inexpensive tool for phenotyping, is widely used in small animal imaging.

In this work, we apply micro cone beam CT for small animal lung imaging *in vivo*. Since the lung is a moving object, motion artifacts, which are detrimental to any tomographic imaging technique[12-14], have to be compensated for to obtain accurate reconstructions. Different schemes have been designed to reduce the motion artifacts when we scan a moving object. The first approach is to do an ultrafast scanning so that the motion can be frozen in time[15]. But since small animals are breathing at a very high rate, about 100 cycles per second for rats, this ultrafast scanning is difficult to achieve in existing micro CT scanners. The second method is to do a corrective reconstruction in which the motion is modeled in the reconstruction algorithm[16,17]. However, this method requires that the motion in the chest fit a time varying expansion model, which is usually not satisfied in practice. The third approach is gating. Respiratory gating can be done in real time[18]. Whenever the lung is in a specific phase of ventilation, collection of a projection is triggered. This real time gating needs an experimental set up to monitor the respiration that could be complicated and interfere the

Medical Imaging 2004: Physiology, Function, and Structure from Medical Images, edited by Amir A. Amini, Armando Manduca, Proceedings of SPIE Vol. 5369 (SPIE, Bellingham, WA, 2004) · 1605-7422/04/$15 · doi: 10.1117/12.535900

natural respiration of the animal. We call this real time gating scheme as the traditional method. In this work, we propose and implement a post acquisition lung gated imaging method that does not require monitoring respiration during data collection. Instead of collecting one projection per view angle in normal tomographic scanning, we collect a projection sequence for each view angle and achieve the gated reconstruction by utilizing the respiratory phase information encoded in the projection sequence. The fundamental idea is that the change of lung volume can be detected by the change of integrated intensity within a ROI around the lung in the projections. By applying our gating method, different phases of the breathing cycle can be reconstructed from one tomographic scan. Our post acquisition lung gated imaging may find applications in lung tumor detection, dynamic pulmonary physiology studies and the respiratory systems modeling.

2. METHODOLOGY

2.1 Image Collection

Although the gating method proposed in this work can be applied to various small animal models, we use rats as our subjects. Sprague-Dawley rats with body weight of 350-400 grams were anesthetized (40mg/kg sodium pentobarbital, ip), placed upright in a plastic cylinder, suspended by restraints attached to the forelimbs and teeth. The cylinder is mounted on a micromanipulator stage for imaging (Fig. 1). The micro-focal x-ray CT system is composed of a Fein-Focus-100.50 x-ray source (3um focal spot), a North American Imaging AI-5830-HP image intensifier coupled to a Silicon Mountain Design (SMD) CCD, and a New England Affiliated Technologies specimen micromanipulator stage all mounted on a precision rail with position information provided by Mitutoyo linear encoders. The geometry of the imaging system allows magnification of the specimen to be adjusted by changing the specimen's proximity to the x-ray source. For each of the 360 viewing angles for which data was acquired, we continuously collect a sequence of images at 30 frames per second for 3 seconds. During this sequence, the rat completes multiple breaths. It should be noted that each of these projections has a relatively low signal-to-noise ratio, see Fig. 2(a), since we do not average multiple frames to get a projection. Averaging over consecutive frames is a common practice when imaging a stationary object to improve the signal-to-noise ratio. The image data (512x512 pixels, 8 bits per pixel) is sent from the CCD to a frame grabber board mounted in a Dell 610 workstation running the WindowsNT operating system. Image acquisition, recording positional information and stage control is each preformed by custom written in-house window based software running on the workstation. The data is then transferred via network to a Red Hat Linux based Dell 410 workstation and after proper preprocessing of the projection images to compensate for distortions introduced by the imaging chain, isotropic reconstructions are obtained through an implementation of the Feldkamp cone-beam algorithm[19].

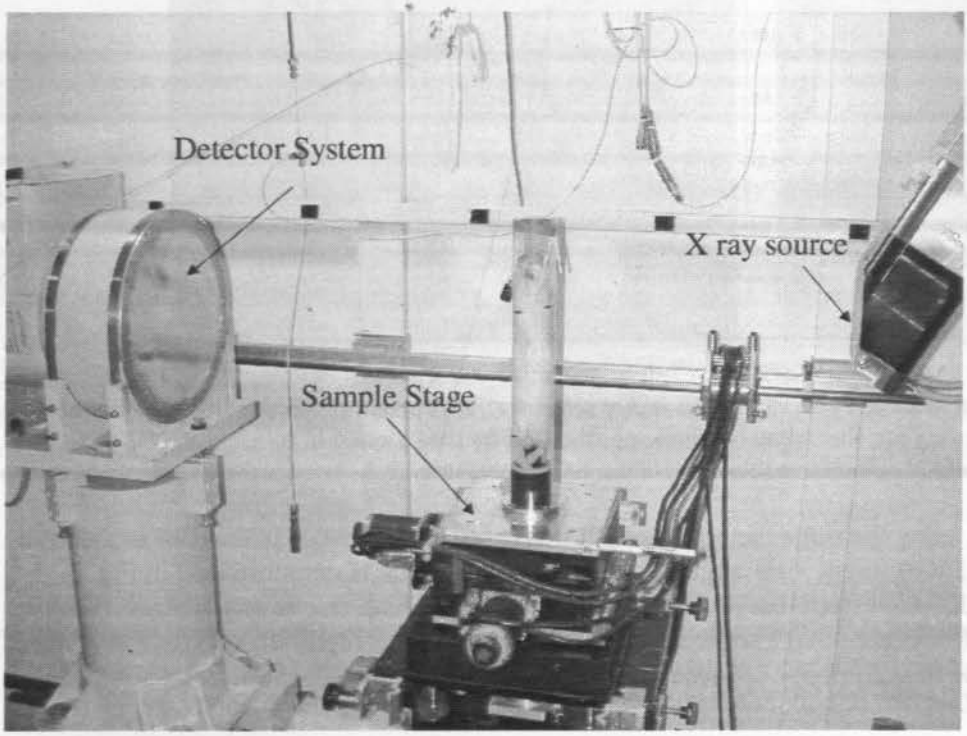

Fig. 1 Experimental setup. The rat suspended upright in a plastic cylinder that is mounted on the specimen stage. The detector, on the left, is a North American Imaging image intensifier coupled to a Silicon Mountain Design CCD camera. The micro-focal x-ray source, on the right, is a Fein-Focus 100.50. The position of the detector and specimen stage are adjustable with respect to the source.

2.2 Respiratory Curve

For each image sequence collected from a specific angle, we have a corresponding periodic respiratory curve which changes with different phases of the breathing cycle. This signal will be used in the gated imaging. The respiratory curve can be obtained by measuring the intraesophageal pressure while collecting the projection image since the pressure changes with different phases of the breathing cycle. However, this pressure measurement process is complicated and could affect the natural breathing of small animals. Instead, we obtain the respiratory curve from the image sequence itself. The idea is as follows. If we have a region around the lung (the white box in Fig. 2(a)) in the projection image, then the total intensity within the region will change throughout the breathing cycle. When the lung is deflated, less air and more soft tissue are projected into the region and the total intensity within the region will be low. Conversely, when the lung is inflated, more air and less soft tissue are projected into the region and the total intensity will be high. Thus a respiratory curve showing different phases of the lung can be obtained (Fig.2 (b)). Note that every point in the curve corresponds to an image. We have the following advantages in obtaining the respiratory curve in this manner:

1. No additional experimental complexity monitoring the respiration, threshold detection and triggering the capture of a projection image
2. Synchronization of the image and ventilation signal is essentially automatic, since the phase information is encoded in the projection itself

The disadvantages are a largely increased collected data set size and the absence of data on intrapleural pressure, which is required in some pulmonary physiology studies. For example, in a compliance study, we have to know both volume and pressure information.

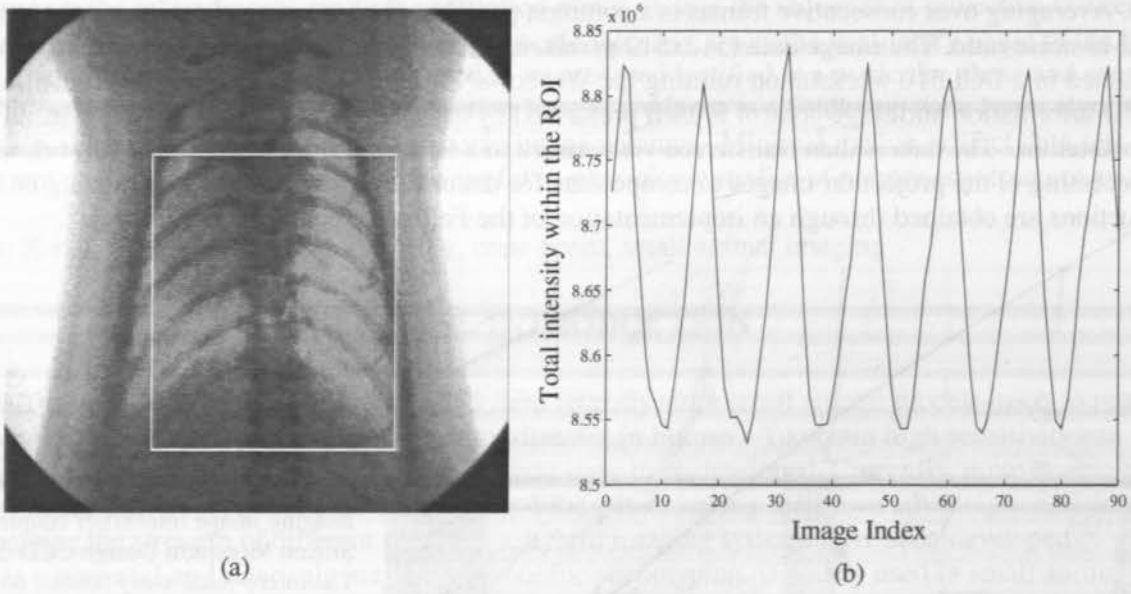

Fig.2 Illustration of the processes of obtaining a respiratory curve from an image sequence. a) A planar projection image of the thorax region in a Sprague-Dawley rat. The white box indicates the ROI for data plotted in b.
b) A plot of the cumulative intensity for the ROI shown in a.

Likewise, we can obtain a breathing curve using the same method for each image sequence. Because the data is acquired asynchronously, breathing curves obtained at different view angles are out of phase, which is demonstrated in Fig. 3. The starting point of curve 1(Fig. 3(a)) is different from that of curve 2(Fig. 3(b)). Therefore, movement artifacts result if we take a projection with the same index from each image sequence and perform the tomographic reconstruction. Fig. 4 shows a reconstruction from the first frame of each image sequence. Motion artifacts are present in the reconstructed

image. The edge of the lung is very blurry and the ribs are not well defined. In addition, the signal to noise ratio in the reconstruction is low, since the projection from each angle is formed by a single frame only.

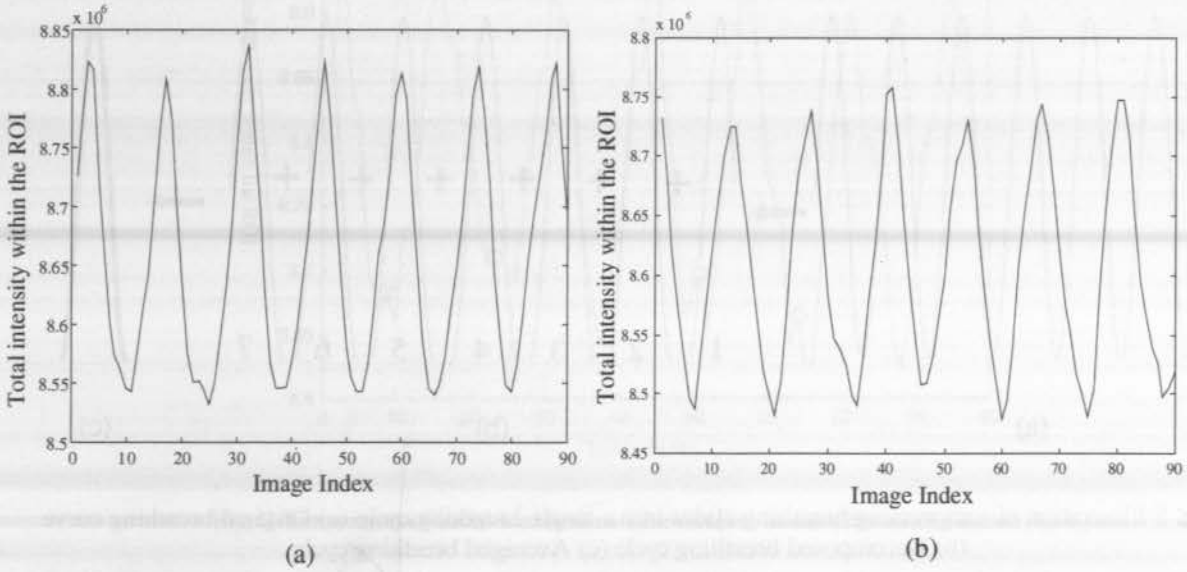

(a) (b)

Fig. 3 Respiratory curves from two different view angles

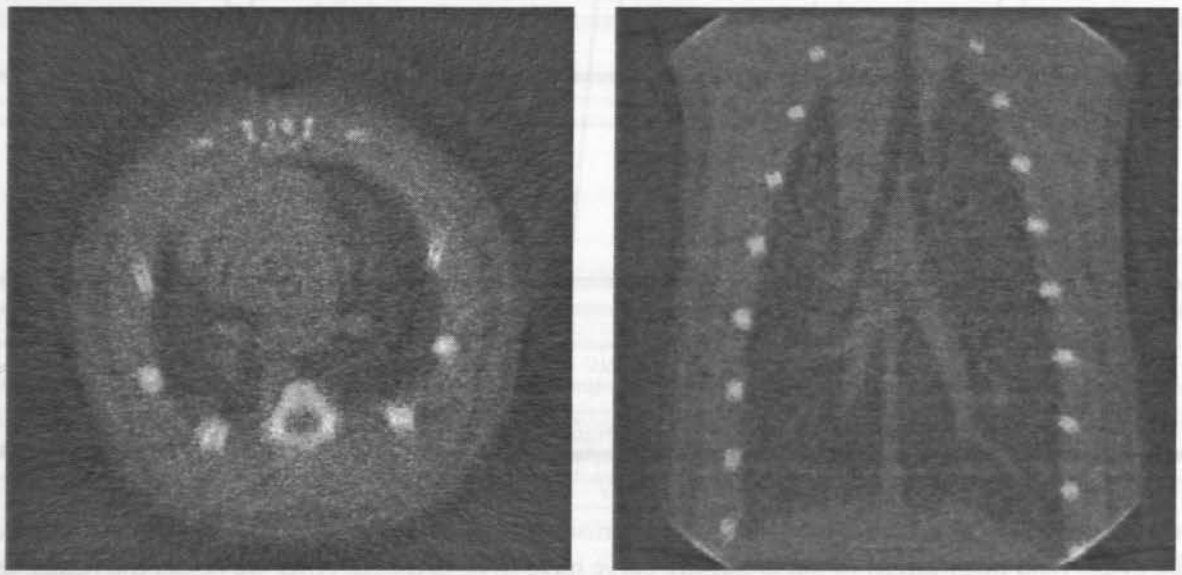

(a) (b)

Fig. 4 Reconstruction without gating (a) Transaxial Image (b) Coronal Image

2.3 Post Acquisition Gating

The key of performing gated pulmonary imaging is to make every image sequence in phase. Our approach to achieve the above goal is to compress the image sequence that contains multiple breathing cycles into a single cycle by decomposing and averaging (Fig. 5). Fig. 5 (a) shows an original breathing curve containing several cycles. In Fig. 5 (b), the breathing curve is decomposed into several complete breathing cycles (2-6) and two partial breathing cycles (1 and 7). Fig. 5 (c) is

the averaged complete breathing cycle. Note that the partial breathing cycles can also be used in the averaging. After obtaining averaged, ordered projection images for a complete breath for every projection angle, we can identify projections with the same index from different view angles and perform a tomographic reconstruction (Fig. 6). Thus the motion artifacts can be reduced.

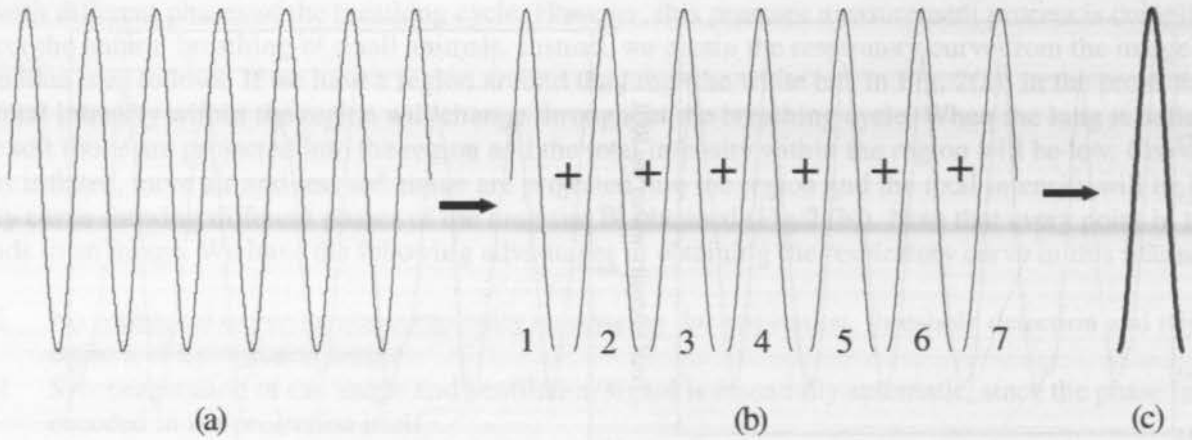

Fig. 5 Illustration of compressing breathing cycles into a single breathing cycle (a) Original breathing curve (b) Decomposed breathing cycle (c) Averaged breathing cycle

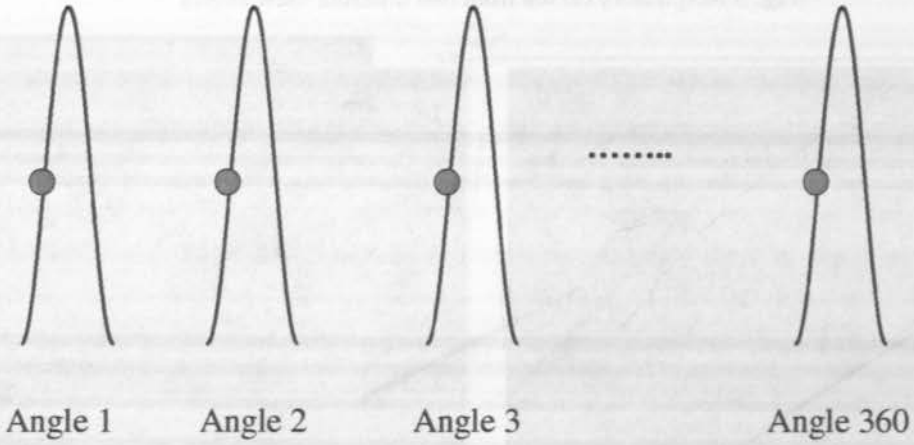

Fig. 6 The same point in a breath cycle must be used from each viewing angle to obtain a reconstruct from that particular phase.

A regular ventilation cycle can be defined by its peak and period. In order to decompose the original breathing curve, the locations of the peaks (end inspiration) in the breathing curve have to be detected. After we detect the peaks, the length of the cycle can be estimated by calculating the average distance between the peaks. If the respiratory curve is homogeneous and noiseless, as shown in Fig. 5(a), then decomposition of the breathing curve will be easy to achieve. However, anomalies in the curve will complicate the peak detection process. These anomalies include local maximums and peaks corresponding to a sigh (deep breath).

Local maximums (circled points in the Fig. 7) are often present in the breathing curve. They are caused by the heart beating and the noise in the projections. These local maximums can be eliminated using the following approach:

1. Estimate the length of the breathing cycle.
2. There is only one true maximum in the window of one breathing cycle, local maximums do not meet this criterion.

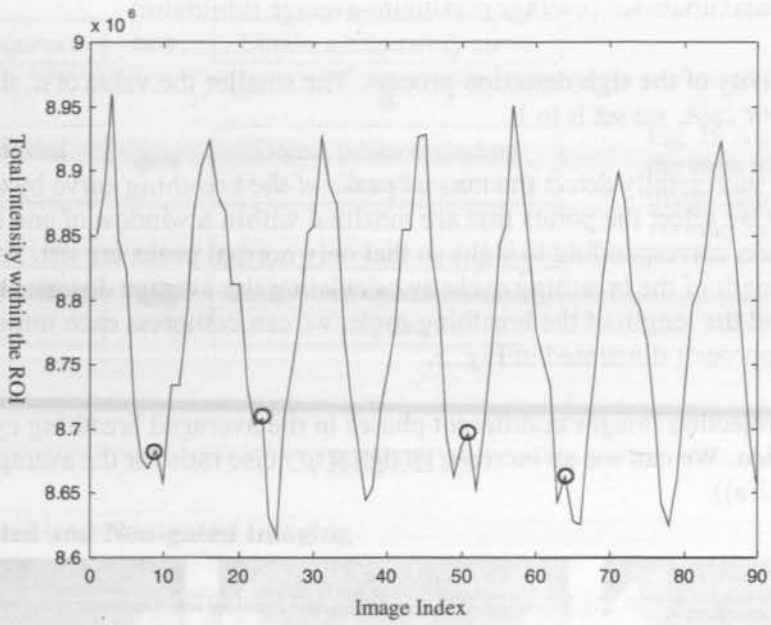

Fig. 7 Illustration of local maximums (the circles) in the respiratory curve

When the rat sighs, the volume of the lung changes dramatically and a large peak appears in the breathing curve (Fig. 8). Since the volume change corresponding to the sigh is different from that of normal breaths, the images corresponding to the sigh should be eliminated in the gated imaging.

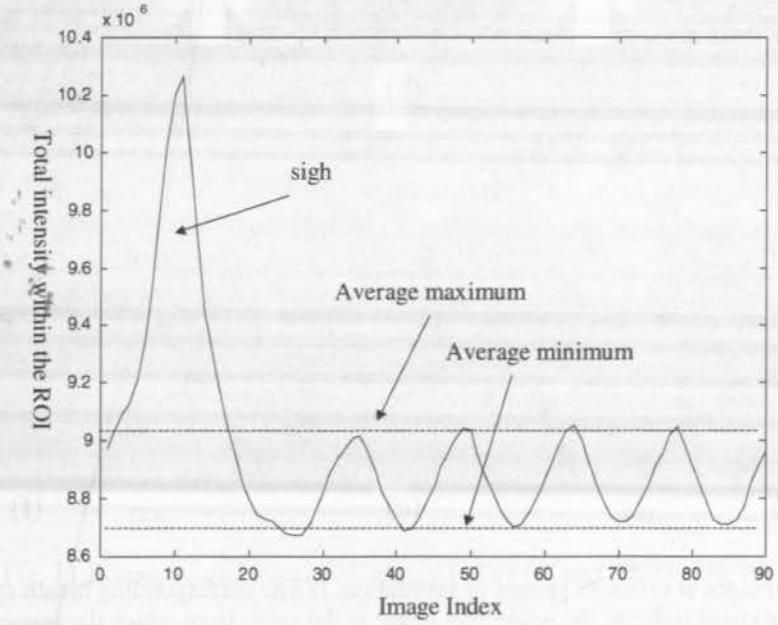

Fig. 8 Illustration of a respiratory curve that includes a sigh (deep breath) during the acquisition sequence

Empirically, we know that sighs occur infrequently and can assume that there exists at most only one sigh in each image sequence. To detect the cycle corresponding to the sigh in the breathing curve, we use the following 4-step approach.

1. Calculate the average maximum excluding the largest maximum since it may be caused by a sigh.
2. Calculate the average minimum
3. Calculate the distance between average maximum and average minimum.
4. The maximums which satisfy the following criterion are caused by sighs

maximum>average maximum+a · (average maximum-average minimum)

where a determines the sensitivity of the sigh detection process. The smaller the value of a, the more sensitive the detection process will be. In our case, we set it to 1.

From above analysis, we can successfully detect the normal peaks of the breathing curve by using the method that is generalized as follows. Firstly we select the points that are maximal within a window of one breathing cycle as peaks. Secondly we eliminate the peaks corresponding to sighs so that only normal peaks are left. After we detect the normal peaks, we can calculate the length of the breathing cycle by calculating the average distance between them. By knowing the locations of maximums and the length of the breathing cycle, we can compress each image sequence into one averaged cycle by using the approach illustrated in Fig. 5.

Fig. 9 shows representative projection images at different phases in the averaged breathing cycle, with phase (c) corresponding to end inspiration. We can see an increase in signal to noise ratio for the averaged projections compared to the original projections (Fig. 2(a)).

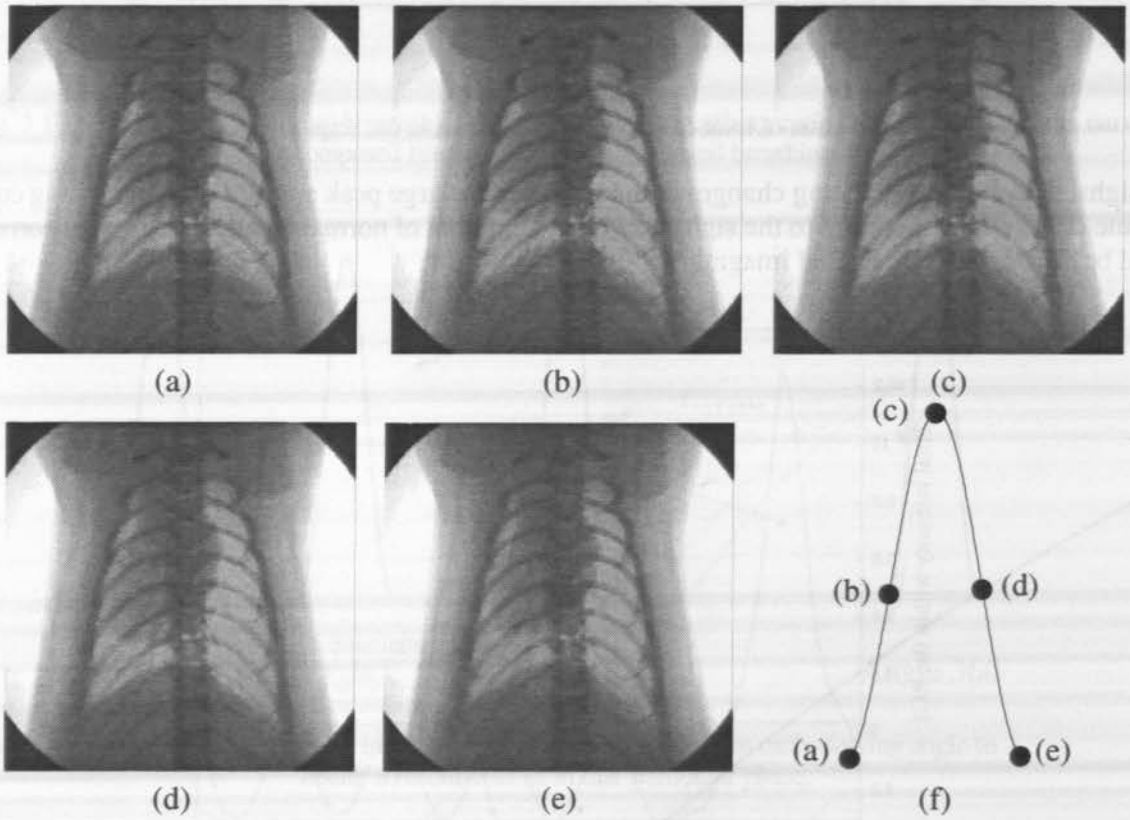

Fig. 9 a-e) Averaged projection images at different phases of ventilation. f) The corresponding breath cycle for the projection images. The points along the curve indicate the respective phase in the cycle from which the images were obtained.

In summary, the processing of each original image sequence collected from different view angles is illustrated in the following diagram (Fig. 10).

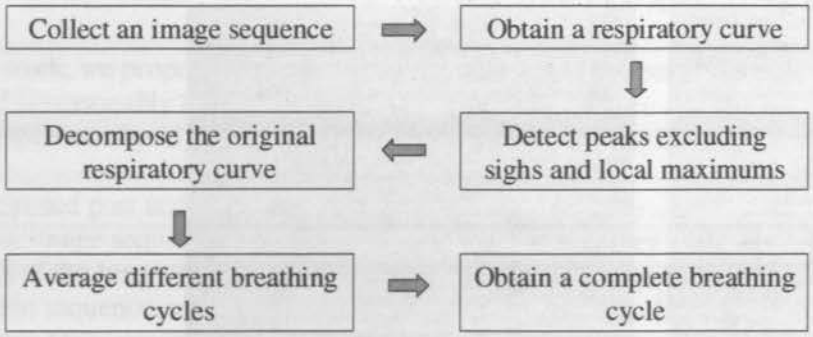

Fig. 10 A schematic diagram showing the steps required to process the image sequence collected at each viewing angle.

3. RESULTS

3.1 Comparison of Gated and Non-gated Imaging

Fig. 11 shows a comparison between reconstructed transaxial images before (a) and after (b) gating. Fig. 12 shows a comparison between reconstructed coronal images before (a) and after (b) gating. An improvement in the image quality after gating is clearly evident in these two figures. In the gated reconstruction, registration of the bone is much better, the edge of the lung is clearly defined and structures within the lung parenchyma are better resolved.

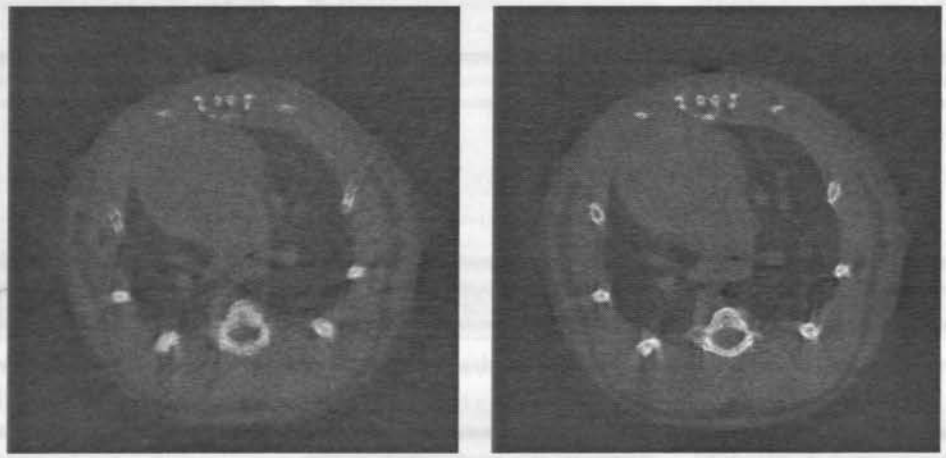

(a) (b)

Fig. 11 Reconstructed transaxial images before (a) and after gating (b)

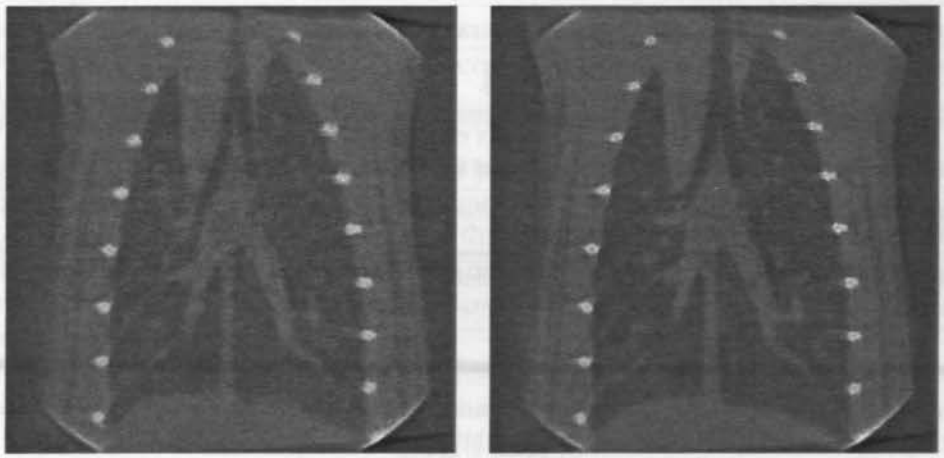

(a) (b)

Fig. 12 Reconstructed coronal images before (a) and after gating (b)

3.2 Phase Reconstruction of the Breathing Cycle

A true advantage of our technique is that different phases of the ventilating lung can be reconstructed from a single scan, which is helpful in performing dynamic pulmonary studies. Fig. 13 shows reconstructed transaxial images at different phases (a,b,c,d,e) within a ventilation cycle, with phase (c) corresponding to maximal inspiration. From multi-phase reconstructions, the changes of the airways and other structures within the lung can be identified while the rat is breathing. This information is important in developing a dynamic model for the respiration system[20].

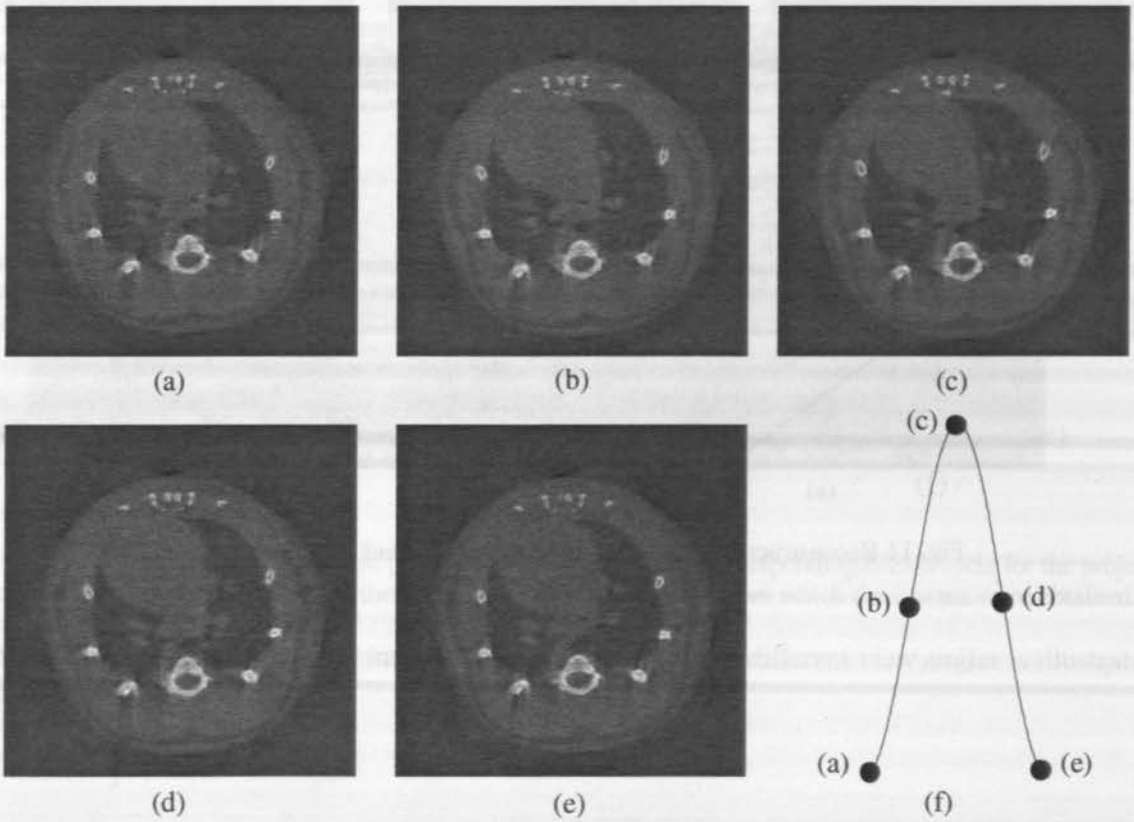

Fig. 13 a-e) Transaxial reconstructions at different phases of the ventilation. f) The corresponding breath cycle for the reconstructed transaxial images. The points along the curve indicate the respective phase in the cycle from which the images were obtained.

4. CONCLUSIONS AND DISCUSSION

In this work, we propose and implement a post acquisition gating method for small animal lung imaging *in vivo*. This method is reasonably easy to implement and does not require additional experimental setup to monitor the respiration. The ventilation signal, which is necessary for the gated imaging, is essentially encoded in the image sequence itself.

The proposed post acquisition gated imaging method can be summarized as follows: For each view angle, we collect a low dose image sequence which contains multiple respiratory cycles. Subsequently, the respiratory curve reflecting changes of the lung volume is obtained by tracing the change of total intensity within an ROI around the lung in the projection sequence, which is then compressed into one breathing cycle by using a decomposing and averaging technique. Once we obtain a complete breathing cycle for each view angle, we can use the projection with the same index from different view angle and do the tomographic reconstruction. Motion artifacts can thus be reduced. In obtaining the respiratory curve, care should be taken for the choice of the ROI in the projection images. Since the diaphragm is the major muscle in normal tidal breathing, it is important to include the diaphragm in the ROI to get a respiratory curve which truly reflects the pattern of the lung volume change. If we do not include the diaphragm in the ROI, the curve we obtain can be misleading and the proposed gating method may not work.

One major disadvantage of the proposed algorithm is that it requires a large amount of data storage space. In normal data collection, we usually average the projections on the fly in memory first, and then store the final averaged projections on the hard drive. However, in the proposed method, we have to store every projection frame the CCD camera captured on the hard drive for post acquisition processing. This leads to a large increase in storage requirements. For example, for a normal scan of 360 views, we need 360*512*512=94 Mbytes storage space. But for a dynamic scan proposed in this work, we need 360*512*512*90=8.4 Gbytes of storage space. However, with our proposed scanning method, multiple phases in a breathing cycle can be reconstructed from a single scan, which is usually not achievable by standard gating methods. Dosage/exposure time is another concern for the proposed algorithm. If the goal is to image the entire breathing cycle, the dosage is no higher than normal methods. However, if we only image one phase in the breathing cycle, then the traditional gating method will result in a lower dosage than that of the proposed algorithm.

ACKNOWLEDGEMENTS

This work is supported by HL 19298, NSF BES 9818197, the W.M. Keck Foundation and the Department of Veterans Affairs.

REFERENCES

1. Paulus MJ, Gleason SS, Easterly ME and Foltz CJ, "A review of high resolution x-ray computed tomography and other imaging modalities for small animal research", *Lab Animal* vol. 30 pp.36-45, 2001
2. Johnson GA *et al* "Nuclear magnetic resonance imaing at microscopic resolution", *Journal of Magnetic Resonance* vol. 68 pp. 129-137, 1986
3. Weber DA, Ivanovic M, Franceschi D *et al*, "Pinhole SPECT: an approach to in vivo high resolution SPECT imaging in small laboratory animals", *Journal of Nuclear Medicine* vol. 35 pp. 342-348, 1994
4. Tsui BMW, Wang Y; Yoder BC, Frey EC, " Micro-SPECT", *Proceedings of IEEE International Symposium on Biomedical Imaging*, pp 373 – 376, 2002
5. Cherry SR, Shao Y, Silverman RW, *et al*, "Micro PET: A high resolution PET scanner for imaging small animals", *IEEE Transactions on Nuclear Science* vol. 44 pp. 1161-1166, 1997
6. Paulus MJ, Gleason SS, Kennel SJ, Hunsicker PR and Johnson DK, "High resolution X-ray computed tomography: An emerging tool for small animal cancer research", *Neoplasia* vol.2 pp. 62-70, 2000
7. Karau KL, Johnson RH, Molthen RC, *et al* "Microfocal x-ray CT imag-ing and pulmonary arterial distensibility in excised rat lungs",*American Journal of Physiology (Heart Circ.Physiol.)*, Vol.281. pp.1447-1457, 2001.
8. Wang G and Vannier MW, ''Micro-CT scanners for biomedical applications:an overview'', *Adv. Imaging* vol.16, pp. 18–27, 2001

9. Bentley MD, Ortiz MC, Ritman EL and Romero JC "The use of microcomputed tomography to study microvasculature in small rodents" *American Journal of Physiology (Regulatory Integrative Comp Physiol)*, vol. 282, pp1267-1279, 2002
10. Hasegawa BH, Iwata K, Wong KH, Wu MC, Da Silva AJ, Tang HR, Barber WC, Hwang AH, Sakdinawat AE, "Dual-modality imaging of function and physiology" *Academic Radiology* Vol. 9 pp. 1305-21, 2002
11. Weisenberger A, Wojcik R, Bradley E *et al* "SPECT-CT System for small animal imaging" *IEEE Trans. Nuclear Science* vol. 50 pp 74-79,2003
12. Godwin J, Breiman R and Speckman J, "Problems and pitfalls in the evaluation of thoracic dissection by computed tomography" *Journal of computer assisted tomography* vol. 6 pp. 750-756, 1982
13. Segars WP and Tsui BMW, "Study of the efficacy of respiratory gating in myocardial SPECT using the new 4-D NCAT phantom" *IEEE Transactions on Nuclear Science*, Vol 49 2002 pp 675 – 679
14. Tsui BMW, Segars WP and Lalush DS, " Effects of upward creep and respiratory motion in myocardial SPECT" *IEEE Transactions on Nuclear Science*,Vol. 47 pp.1192 – 1195, 2000
15. Goldberg H, Gould R, Feuerstein I, Sigeti J and Lipton M, "Evaluation of ultrafast CT scanning of the adult abdomen", *Investigative Radiology* vol. 24 pp 537-543,1989
16. Crawford C, King K, Ritchie C and Godwin J "Respiratory compensation in projection imaging using a magnification and displacement model", *IEEE Transactions on Medical Imaging* vol. 15 pp. 327 –332, 1996
17. Ritchie CJ, Crawford CR, Godwin JD, King KF and Kim Y, "Correction of computed tomography motion artifacts using pixel-specific back-projection", *IEEE Transactions on Medical Imaging* vol. 15 pp. 333 –342,1996
18. Ritchie C, Hsieh J, Gard M, Crawford C and Kim Y "Predictive respiratory gating: A new method to reduce motion artifacts in CT scans" *Radiology* vol. 190 pp. 847-852, 1994
19. Feldkamp LA, Davis LC and Kress JW "Practical cone-beam algorithm", *J. Opt. Soc. Am. A* vol.1, pp. 612-619, 1984
20. Garrity JM, Segars WP, Knisley SB and Tsui BMW "Development of a dynamic model for the lung lobes and airway tree in the NCAT phantom", *IEEE Transactions on Nuclear Science* ,Vol. 50 pp. 378 – 383, 2003